Hybrid Modeling and Control of a Robotic Arm with Contact Detection

Julio Quiroga Galan
Department of Electrical and Computer Engineering
University of California, Santa Cruz
ECE 246: Hybrid Dynamical Systems
Professor Ricardo G. Sanfelice
Email: jquirog@ucsc.edu

***Abstract*—This paper presents the hybrid modeling and control of a robotic arm operating under two control modes: position control and force control, depending on contact interaction. The hybrid system is modeled using state-triggered logic, simulated in MATLAB, and analyzed for solution behavior and performance.**

I. Introduction

In many robotic manipulation tasks, physical interaction with the environment plays a critical role. Robotic arms often operate in settings that require alternating between free motion and constrained motion, such as during assembly, packaging, or object manipulation. These interactions naturally introduce abrupt transitions in the system's dynamics such as, when an arm makes or breaks contact with a surface, leading to challenges in control design, stability analysis, and real-time execution. Traditional continuous-time models are not well-suited to handle such discrete, event-driven changes, motivating the need for hybrid dynamical modeling.

The goal of this project is to model and control a robotic arm performing a sequence of tasks that includes approaching an object, establishing contact, regulating contact force, and releasing the object through a throwing motion. Modeling this system using hybrid dynamics enables the explicit representation of both continuous evolution (e.g., position and velocity under control) and discrete transitions (e.g., switching control modes based on contact conditions).

Contact detection presents a key challenge, as naive switching between modes based solely on threshold crossing can lead to undesirable chattering or instability due to measurement noise or sensor delays. To address this, we employ hysteresis-based switching logic inspired by [1], which introduces a pair of thresholds to separate the activation and deactivation conditions. This design ensures robust transitions and avoids rapid toggling between control modes.

We adopt the modeling framework proposed in [1], which provides a simplified but effective abstraction for contact-interacting robotic systems. While alternative modeling approaches such as, purely event-driven controllers or high-fidelity contact models with friction and compliance. This hybrid formulation facilitates stability analysis using Lyapunov methods, and naturally integrates logic-based control strategies such as mode-dependent dynamics and resets.

The remainder of this paper details the development of the hybrid model, its numerical simulation in MATLAB using the HyEQ Toolbox [2], and an analysis of the system's behavior and stability under the proposed control scheme.

II. Methodology

A. System Description and Physical Setup

We consider a robotic arm with one degree of freedom constrained to motion along a horizontal axis. The arm interacts with a compliant environment modeled using a Kelvin-Voigt [1] contact model. The task consists of three phases: (i) free motion until contact with the environment is detected, (ii) contact phase where the arm regulates the applied force using a force controller, (iii) throwing phase where the arm releases the object by executing a specific velocity profile, and (iv) resetting the robotic arm to its original location.

The compliant surface is described using a linear spring and damper system, defined by stiffness k_c and damping b_c, respectively. This setup closely follows the modeling approach described in [1], where the contact detection relies on measured forces and transitions are governed by hysteresis thresholds.

B. State Variables and Parameters

We define the continuous state vector $x = [x_1 \;\; x_2]^\top \in \mathbb{R}^2$, where x_1 represents the angular position and x_2 the angular velocity of the robotic arm's. The full hybrid state is $z = [x_1 \;\; x_2 \;\; q]^\top$, where $t \in \mathbb{R}_{\geq 0}$ is a time-keeping variable used for simulation and $q \in \{0, 1, 2, 3\}$ is a discrete state representing the current control mode.

The parameters governing the system dynamics are as follows. The proportional and derivative gains used in the position control mode are $k_p, k_d \in \mathbb{R}_{\geq 0}$. During force control, the system applies feedback with gain $k_f \in \mathbb{R}_{\geq 0}$, aimed at tracking a desired contact force $f_d \in \mathbb{R}_{>0}$. The interaction with the environment is modeled using a Kelvin–Voigt contact model with stiffness $k_c \in \mathbb{R}_{>0}$ and damping $b_c \in \mathbb{R}_{>0}$. Transitions between contact and non-contact modes use one hysteresis thresholds: $\gamma \in \mathbb{R}_{>0}$ for entering contact. A tolerance band $\delta \in \mathbb{R}_{>0}$ is used to avoid chatter during force convergence, such that transitions occur when the contact force $f_c \in [f_d - \delta, \; f_d + \delta]$.

The throwing phase is implemented using a sinusoidal forcing input of amplitude $A \in \mathbb{R}_{>0}$ and frequency $\omega \in \mathbb{R}_{>0}$. The transition to ballistic motion occurs when the velocity exceeds a release threshold $v_{\text{release}} \in \mathbb{R}_{>0}$. During ballistic motion, the acceleration due to gravity is modeled using $g \in \mathbb{R}_{>0}$. Finally, $x_d \in \mathbb{R}$ denotes the desired angular position used in the position control objective during mode $q = 0$.

C. Hybrid System Modeling

The hybrid behavior of the robotic arm is modeled through a state-triggered system with four discrete modes $q \in \{0, 1, 2, 3\}$, each representing a distinct control phase: position control, force control, throwing, and ballistic reset.

We define the hybrid system:

$$\mathcal{H} := \begin{cases} z \in \mathcal{C}, & \dot{z} = f(z) \\ z \in \mathcal{D}, & z^+ = g(z) \end{cases}$$

where $z = [x_1,\ x_2,\ q]^\top \in \mathbb{R}^2 \times \{0, 1, 2, 3\}$ is the hybrid state vector including position, velocity, time, and discrete mode.

Flow Map $f(z)$: The continuous dynamics are mode-dependent:

$$f(z) = \begin{cases} [x_2;\ u - f_c(x_1, x_2);\ 0]^\top, q = 0 & \text{(Position control)} \\ [x_2;\ k_f(f_d - f_c(x_1, x_2));\ 0]^\top, q = 1 & \text{(Force control)} \\ [x_2;\ A\sin(\omega t);\ 0]^\top, q = 2 & \text{(Throwing)} \\ [x_2;\ -g;\ 0]^\top, q = 3 & \text{(Reset)} \end{cases}$$

The contact force is defined by the Kelivin-Voigt model [1]:

$$f_c(x_1, x_2) = \begin{cases} k_c(x_1 + 0.05) + b_c x_2, & \text{if } x_1 \geq -0.05 \\ 0, & \text{otherwise} \end{cases}$$

Control Logic Justification: The control input u is designed to match the operational goals of each mode:

- **Mode $q = 0$ (Position Control)**: The arm is not in contact with the environment. A PD (Proportional-Derivative) controller is used to drive the end-effector toward a desired position x_d. The control law

  $$u = -k_p(x_1 - x_d) - k_d x_2$$

  ensures that the arm decelerates as it approaches the target and avoids overshooting by damping its velocity. This is suitable for free-space motion before contact is made.
- **Mode $q = 1$ (Force Control)**: Contact has been established. The goal now is to regulate the contact force f_c to match a desired value f_d. To achieve this, the controller introduces a feedback term:

  $$u = f_c + k_f(f_d - f_c)$$

  The term f_c cancels the environment's stiffness and damping effects (via feedback linearization), while $k_f(f_d - f_c)$ ensures convergence of the actual force to the desired target.
- **Mode $q = 2$ (Throwing)**: Once the desired contact force has been maintained, the arm executes a dynamic motion to release the object. The input

  $$u = A\sin(\omega t)$$

  generates a time-varying acceleration profile, mimicking a swing or throw. The parameters A and ω determine the energy and speed of the motion.
- **Mode $q = 3$ (Reset)**: After release, the object is no longer in contact with the arm, and gravity is the only acting force. The arm enters a passive ballistic mode:

  $$u = -g$$

  This causes the system to decelerate and eventually reset once the arm returns to the initial region (e.g., $x_1 \leq -1$). The reset prepares the arm to begin the next manipulation cycle.

Each mode and its corresponding control law are carefully selected to reflect the physical behavior and desired performance of the system under different contact scenarios. This modular control structure ensures smooth transitions, safe interaction with the environment, and reliable repetition of the manipulation task.

Jump Map $g(z)$: The discrete transitions switches the control mode q:

$$g(z) = \begin{cases} [x_1;\ x_2;\ 1]^\top, & q = 0 \wedge f_c(x_1, x_2) \geq \gamma \\ [x_1;\ x_2;\ 2]^\top, & q = 1 \wedge |f_c(x_1, x_2) - f_d| \leq \delta \\ [x_1;\ x_2;\ 3]^\top, & q = 2 \wedge x_2 \geq v_{\text{release}} \\ [-1;\ 0;\ 0]^\top, & q = 3 \wedge x_1 \leq -1 \\ z, & \text{otherwise (no jump)} \end{cases}$$

Flow Set $\mathcal{C}$:

$$\mathcal{C} = \left\{ z \in \mathbb{R}^3 \;\middle|\; \begin{array}{c} (q = 0 \wedge f_c(x_1, x_2) \leq \gamma) \\ \vee\ (q = 1 \wedge |f_c(x_1, x_2) - f_d| \geq \delta) \\ \vee\ (q = 2 \wedge x_2 \leq v_{\text{release}}) \\ \vee\ (q = 3 \wedge x_1 \geq -1) \end{array} \right\}$$

Jump Set $\mathcal{D}$:

$$\mathcal{D} = \left\{ z \in \mathbb{R}^3 \;\middle|\; \begin{array}{c} (q = 0 \wedge f_c(x_1, x_2) \geq \gamma) \\ \vee\ (q = 1 \wedge |f_c(x_1, x_2) - f_d| \leq \delta) \\ \vee\ (q = 2 \wedge x_2 \geq v_{\text{release}}) \\ \vee\ (q = 3 \wedge x_1 \leq -1) \end{array} \right\}$$

D. Well-Posedness of the Hybrid Model

To ensure that the hybrid model is mathematically robust and that its solutions behave predictably, we analyze it under the framework provided in [3]. In particular, we verify that our system satisfies **Assumption 6.5 (Hybrid Basic Conditions)**, and consequently invoke **Theorem 6.8**, which guarantees nominal well-posedness.

a) Verification of Hybrid Basic Conditions::

- **(A1) Closedness of $\mathcal{C}$ and $\mathcal{D}$:** The flow set $\mathcal{C}$ and jump set $\mathcal{D}$ are defined by closed inequalities involving the state variables (e.g., $x_1 \geq -0.05$, thresholds on velocity or position, and specific discrete modes). Therefore, both sets are closed subsets of $\mathbb{R}^n$, satisfying (A1).
- **(A2) Flow Map F:** The continuous dynamics in each mode ($q = 0, 1, 2, 3$) are defined by smooth functions

(e.g., PD control law, force feedback, sinusoidal input, gravity dynamics). These functions are:
  - Single-valued (not set-valued),
  - Locally bounded (bounded in every compact subset of $\mathcal{C}$),
  - Continuous (and therefore outer semicontinuous),

  This confirms that the flow map F meets all requirements of (A2).
- **(A3) Jump Map G:** The discrete transitions (e.g., from contact to force control, to throwing, to ballistic) are modeled as deterministic state resets, defined as continuous or piecewise continuous maps. These jump rules are:
  - Single-valued and deterministic,
  - Continuous (and therefore outer semicontinuous)
  - Locally bounded relative to the closed jump set $\mathcal{D}$.

  Thus, the jump map G satisfies (A3).

b) Application of Theorem 6.8: Given that the proposed hybrid system satisfies Assumption 6.5, then **Theorem 6.8** from [3], which states that any hybrid system satisfying the hybrid basic conditions is *nominally well-posed*. This means:

- Existence of solutions is guaranteed for any initial condition in $\mathcal{C} \cup \mathcal{D}$.
- Solutions depend continuously on initial conditions.
- There are no Zeno phenomena or ill-defined transitions near the boundaries of $\mathcal{C}$ or $\mathcal{D}$.

III. Solution Types

In the context of hybrid systems, a solution to the hybrid dynamical system $\mathcal{H} = (C, f, D, g)$ is described as a hybrid arc $\phi : \text{dom } \phi \to \mathbb{R}^n$ where dom $\phi \subseteq \mathbb{R}_{\geq 0} \times \mathbb{N}$ is a hybrid time domain, as defined in [3]. This domain allows the system to evolve in both continuous time (flows) and discrete jumps, enabling the modeling of switching dynamics, logic, and resets alongside standard differential equations.

A. Classification of Solutions

According to Definition 2.7 in [3], solutions can be categorized as follows:

- **Complete**: A solution is complete if its domain is unbounded in hybrid time, i.e., $\sup_{(t,j)\in \text{dom } \phi} t = \infty$ or $\sup_{(t,j)\in \text{dom } \phi} j = \infty$.
- **Maximal**: A solution is maximal if it cannot be extended beyond its domain.
- **Zeno**: A solution is Zeno if it has an infinite number of jumps in a finite amount of time.

B. Solutions in the Robotic Arm System

For the robotic arm hybrid system presented in this project, we simulate trajectories under a specific initial condition to analyze the type and behavior of solutions. The evolution follows a repeating sequence of modes:

1) $q = 0$: Free motion under position control
2) $q = 1$: Force control when contact is detected
3) $q = 2$: Throwing motion using a velocity profile
4) $q = 3$: Reset to initial position and mode

Each complete cycle involves both flows (during arm motion and force application) and jumps (when transitioning between control modes). The system resets back to $q = 0$ after $q = 3$, creating an infinite loop of motion.

Given this structure and under the assumption that the force threshold and reset conditions are properly defined, the following observations can be made:

- The solutions observed are **complete**, since the system cycles indefinitely.
- They are also **maximal**, as each solution segment cannot be extended without violating the system's rules.
- The system does **not exhibit Zeno behavior**, since each jump is separated by a strictly positive time interval (i.e., mode transitions do not happen infinitely fast).

IV. Lyapunov Stability

To analyze the stability of the hybrid robotic system, we defined mode-specific Lyapunov candidate functions and studied their evolution along system trajectories. This analysis is grounded in the Lyapunov-based techniques for hybrid systems presented in [3], particularly Section 3.3.

A. Lyapunov Candidate Function for q = 0

During the pre-contact mode, the system operates under a PD controller that drives the angular position of the robotic arm toward a desired target. The closed-loop dynamics are:

$$\dot{x}_1 = x_2, \ \dot{x}_2 \quad = -k_p(x_1 - x_d) - k_d x_2 \tag{1}$$

We propose the kinetic energy formula as the Lyapunov function:

$$V_0(x) = \frac{1}{2}x_2^2 + \frac{1}{2}k_p(x_1 - x_d)^2 \tag{2}$$

This function is positive definite and radially unbounded. The equilibrium set associated with the Lyapunov function $V_0(x)$ is given by:

$$\mathcal{A} = \left\{x \in \mathbb{R}^2 : x_1 = x_d, \ x_2 = 0\right\}$$

This set represents the desired configuration where the robotic arm has reached the target angular position x_d and is at rest. It is the largest invariant set in which $\dot{V}_0(x) = 0$, and thus defines the equilibrium point of the closed-loop system under mode $q = 0$. Its time derivative along system trajectories is:

$$\dot{V}_0(x) = -k_d x_2^2 \leq 0 \tag{3}$$

This confirms that is non-increasing during flows and strictly decreasing when q = 0, establishing Lyapunov stability of the pre-contact configuration.

B. Lyapunov Candidate Function for q = 1

During the force control mode $q = 1$, the objective is to regulate the contact force $f_c(x_1, x_2)$ to match a desired force f_d. The control input in this mode is designed as:

$$\dot{x}_2 = k_f(f_d - f_c(x_1, x_2)) \tag{4}$$

where $k_f \in \mathbb{R}_{\geq 0}$ is a force gain parameter and $f_d \in \mathbb{R}_{\geq 0}$ is the desired contact force. The contact force is given by:

$$f_c(x_1, x_2) = \begin{cases} k_c(x_1 + 0.05) + b_c x_2, & \text{if } x_1 \geq -0.05 \\ 0, & \text{otherwise} \end{cases} \quad (5)$$

To assess convergence to the desired force level, we define a standard quadratic function for the Lyapunov candidate function:

$$V_1(x) = \frac{1}{2}(f_c(x_1, x_2) - f_d)^2 \quad (6)$$

This function is positive definite with respect to the set:

$$\mathcal{A}_1 = \left\{ x \in \mathbb{R}^2 : f_c(x_1, x_2) = f_d \right\} \quad (7)$$

The set $\mathcal{A}_1$ represents the equilibrium configurations in which the actual contact force exactly matches the desired force f_d. The Lyapunov function $V_1(x)$ is minimized and equal to zero on this set.

Taking the time derivative of $V_1(x)$ along flows and assuming $x_1 \geq -0.05$ (i.e., contact is active), we get:

$$\dot{V}_1(x) = (f_c(x_1, x_2) - f_d) \cdot \dot{f}_c(x_1, x_2) \quad (8)$$

From the expression of f_c, its time derivative is:

$$\dot{f}_c = k_c \dot{x}_1 + b_c \dot{x}_2 = k_c x_2 + b_c k_f (f_d - f_c) \quad (9)$$

Substituting into the expression for $\dot{V}_1$, we obtain:

$$\dot{V}_1(x) = (f_c - f_d)(k_c x_2 + b_c k_f (f_d - f_c)) \quad (10)$$

$$\dot{V}_1(x) = (f_c - f_d)(k_c x_2 - b_c k_f (f_c - f_d)) \quad (11)$$

If the velocity term x_2 is small or zero, as is typically expected in force control where motion is slow or stabilized, the dominant term becomes $-b_c k_f (f_c - f_d)^2$, yielding:

$$\dot{V}_1(x) = -b_c k_f (f_c - f_d)^2 \leq 0 \quad (12)$$

This confirms that V_1 is non-increasing along flows in mode $q = 1$ and strictly decreasing whenever $f_c \neq f_d$, verifying Lyapunov stability with respect to the set $\mathcal{A}_1$.

Numerical results shown in Figure 3 and Figure 4 confirm this behavior, with V_1 decreasing during force control and its derivative remaining negative or zero throughout the simulation.

C. On the Absence of Candidates for q = 2

In mode $q = 2$, the system performs a throwing maneuver governed by a sinusoidal control input $u = A\sin(\omega t)$. This input is purposefully designed to inject energy into the system, enabling the robotic arm to achieve a high-velocity release. Unlike modes focused on stabilization or regulation, this phase drives the system away from equilibrium to accomplish a dynamic objective.

Because the system is not intended to converge to any equilibrium during this phase, the fundamental conditions required, that a Lyapunov function should be non-increasing along system trajectories, are inherently violated. Any candidate Lyapunov function would likely increase due to the energy-adding nature of the sinusoidal control.

Therefore, we do not define a Lyapunov function for mode $q = 2$. Instead, we regard this mode as a transient energy-phase that bridges the force regulation and reset behaviors. While its performance is essential for task execution, it falls outside the scope of Lyapunov-based stability analysis.

D. Lyapunov Candidate Function for q = 3

Although mode $q = 3$ represents a passive ballistic phase governed by gravity, its behavior remains structured. The system flows toward a known reset point x_r (e.g., the start of the cycle). Therefore, we define the kinetic energy formula as a Lyapunov candidate centered at the reset target:

$$V_3(x) = \frac{1}{2}x_2^2 + \frac{1}{2}k_p(x_1 - x_r)^2 \quad (13)$$

This function is minimized at $\mathcal{A}_3 = \{(x_1, x_2) \in \mathbb{R}^2 : x_1 = x_r, x_2 = 0\}$, reflecting the system's goal of returning to the start. The time derivative is given by:

$$\dot{V}_3(x) = x_2(-g) + k_p(x_1 - x_r)x_2 \quad (14)$$

$$\dot{V}_3(x) = x_2(-g + k_p(x_1 - x_r)) \quad (15)$$

As the system falls toward x_r, $x_2 < 0$ and $x_1 > x_r$, making $\dot{V}_3(x) < 0$ under typical conditions. Simulation results confirm that V_3 decreases along flows, supporting its role as a valid Lyapunov candidate for this phase.

E. Numerical Verification and Analysis

We simulated the evolution of q=0, q=1, and q=3 using hybrid trajectories generated via the HyEQ Toolbox [2]. Figures 1 and 2 confirm that decreases over time and has a negative derivative during flows in mode q=0. Similarly, Figures 3 and 4 validate the decrease of during mode q=1.

Figures 5 and 6 depict the evolution of in mode q=3. While is not strictly decreasing, it reflects the system's passive return to the initial configuration under gravity. Each jump resets the system, causing a drop in q=3, followed by an increase due to gravitational acceleration. This cyclical energy trend indicates that the system periodically returns to the pre-contact state.

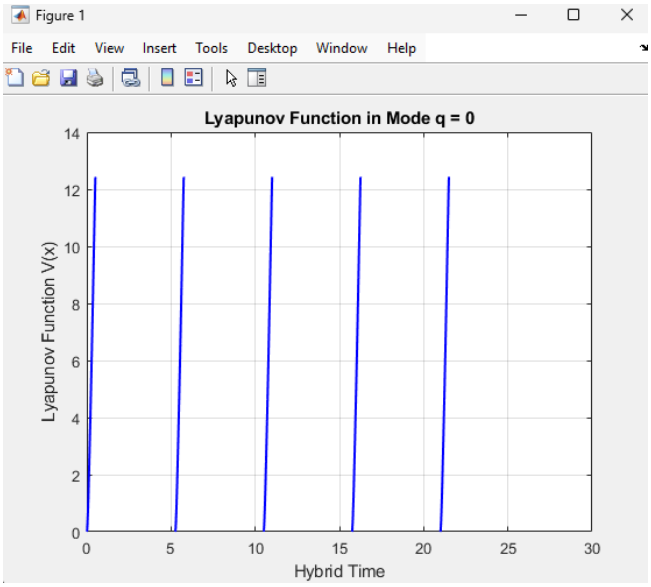

Fig. 1. Lyapunov function during mode q=0

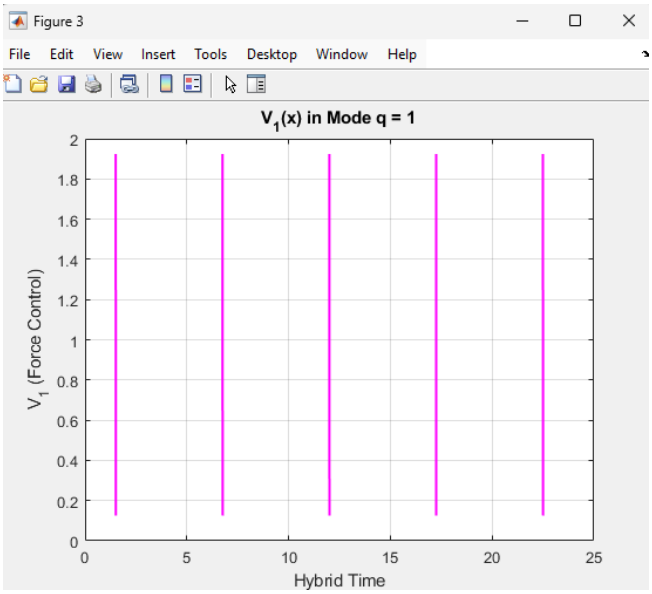

Fig. 3. Lyapunov function during mode q=1

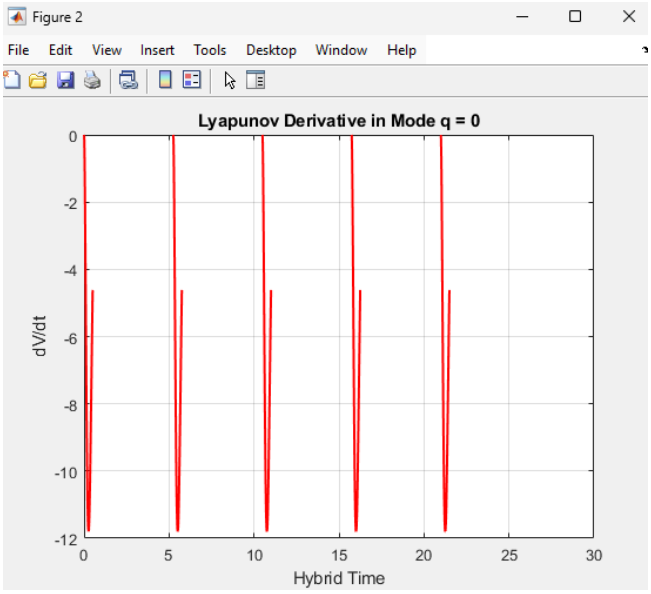

Fig. 2. Time derivative during mode q=0

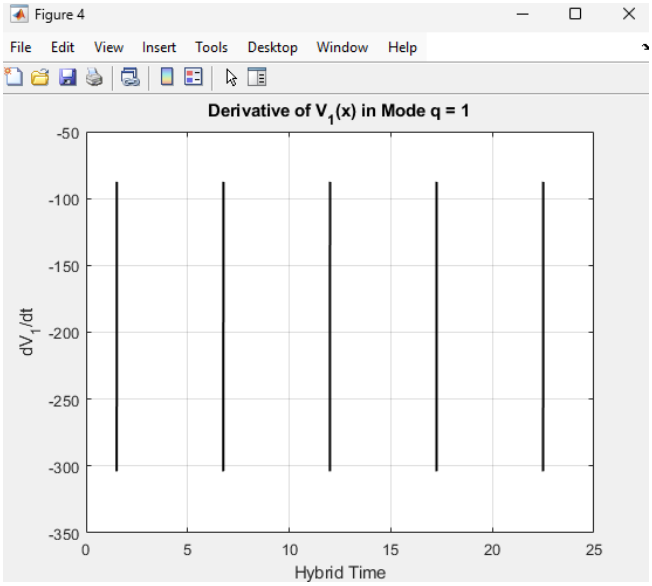

Fig. 4. Time derivative during mode q=1

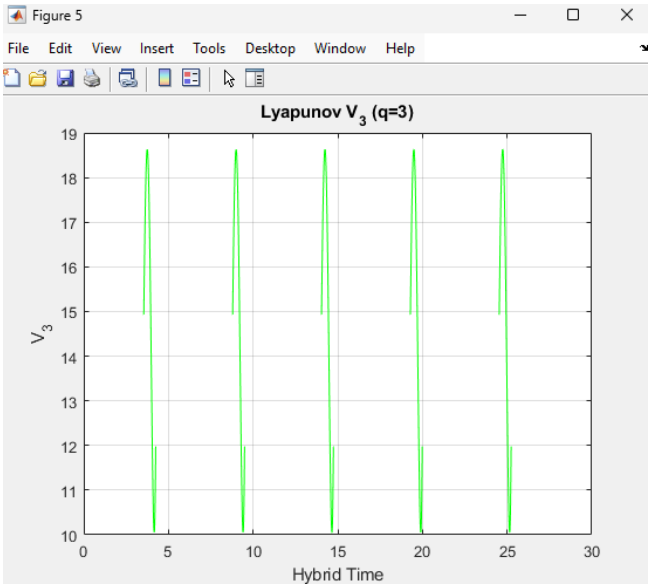

Fig. 5. Lyapunov function during mode q=3

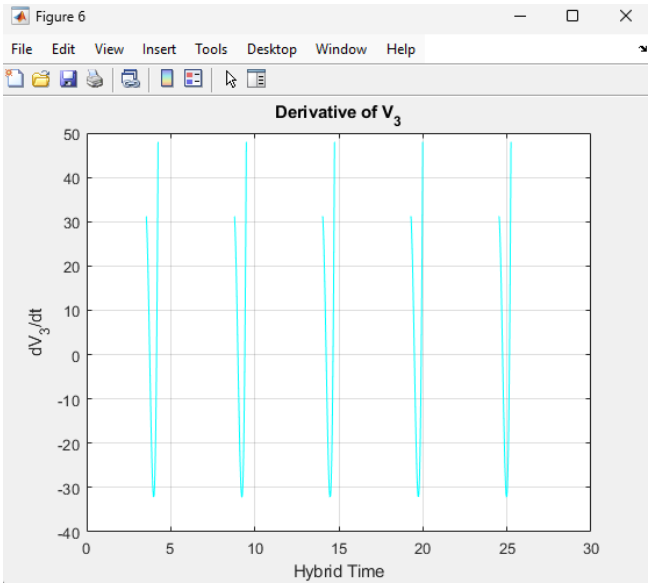

Fig. 6. Time derivative during mode q=3

F. Decrease Across Jump Transitions

In hybrid systems, stability is verified not only through continuous-time behavior but also through discrete jumps between modes. To guarantee asymptotic convergence to a target set, a valid Lyapunov function $V(x)$ must decrease (or at least not increase) across each jump:

$$V(g(x)) - V(x) \leq 0 \quad \text{for all } x \in D,$$

and ideally:

$$V(g(x)) - V(x) < 0 \quad \text{for all } x \in D \setminus \mathcal{A}.$$

To verify this in our system, we implemented a MATLAB-based post-processing of hybrid simulation data. This analysis evaluates the Lyapunov function immediately before and after each jump transition by checking:

$$V^-(x) = V(\phi(t_j, j)) \tag{16}$$

$$V^+(x) = V(\phi(t_j, j+1)) \tag{17}$$

$$\Delta V = V^+(x) - V^-(x) \tag{18}$$

Specifically, we analyzed the transitions from mode $q = 0 \rightarrow q = 1$, which represents a physically meaningful evolution where the system goes from controlled motion to contact-based force tracking. The Lyapunov functions involved were: $V_0(x) = \frac{1}{2}x_2^2 + \frac{1}{2}k_p(x_1 - x_d)^2$ (energy-based), $V_1(x) = \frac{1}{2}(f_c - f_d)^2$ (force tracking error).

The analysis, as shown in Figure 7 and Figure 8, confirms a strict decrease in Lyapunov value across these transitions, satisfying the hybrid Lyapunov condition for this case.

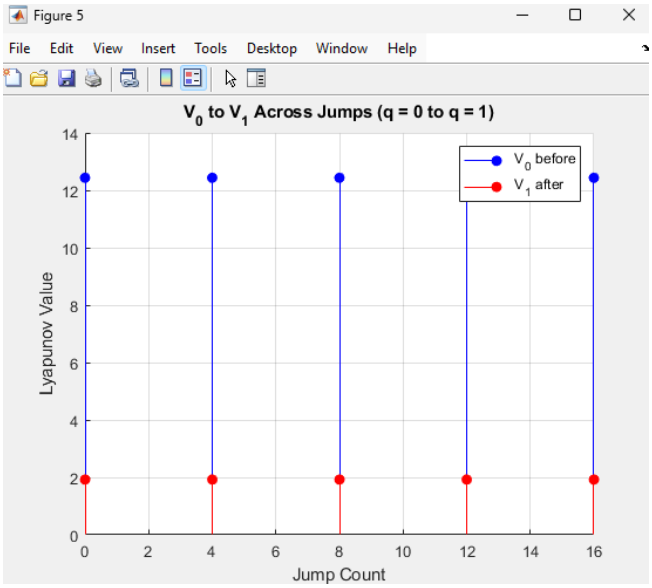

Fig. 7. Values of V before and after jumps from $q = 0$ to $q = 1$.

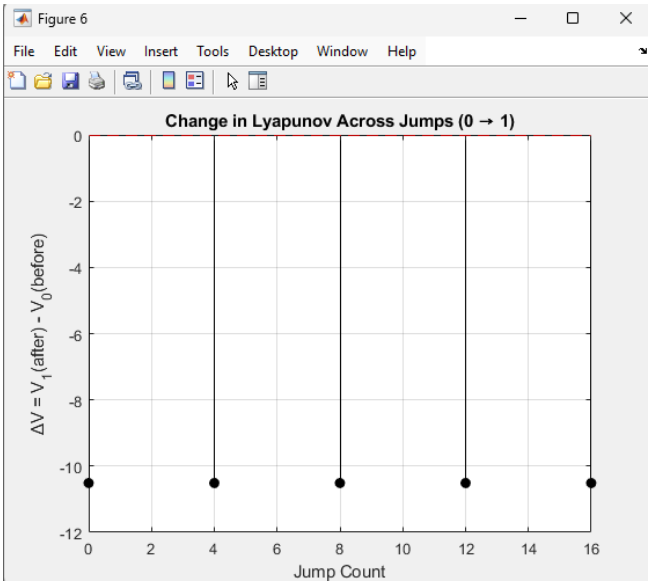

Fig. 8. Change ΔV across jumps $q = 0 \rightarrow q = 1$, showing consistent decrease.

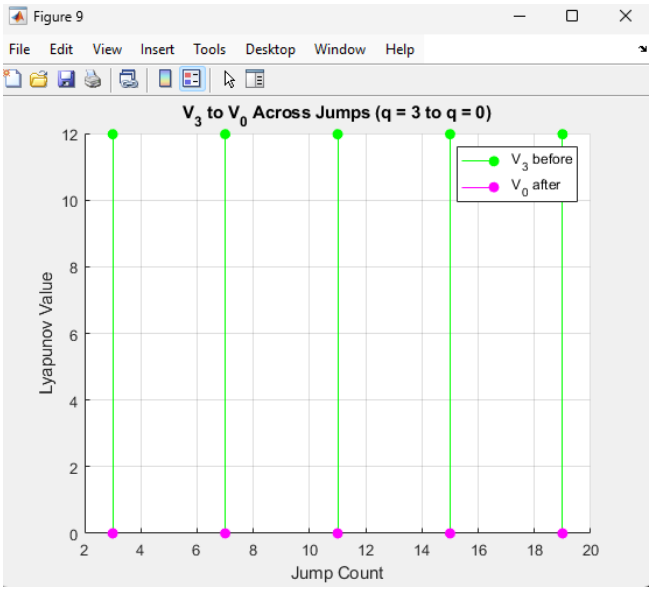

Fig. 9. Values of V before and after jumps from $q = 3$ to $q = 0$.

We did not analyze jumps from $q = 2 \rightarrow q = 3$ because mode $q = 2$ involves a net input of energy through actuation designed to match a desired contact force f_d. Hence, the system may experience a localized energy increase due to external control input, making Lyapunov-based decrease non-guaranteed or not meaningful for that transition.

In addition to the contact transition, we also analyzed the jump from mode $q = 3$ (ballistic phase) to mode $q = 0$ (pre-contact phase). This reset marks the completion of a hybrid execution cycle and the reinitialization of the tracking controller.

Here, the Lyapunov function before and after the jump is of the same structure:

$$V_3(x) = \frac{1}{2}x_2^2 + \frac{1}{2}k_p(x_1 - x_d)^2$$

$$V_0(x) = \frac{1}{2}x_2^2 + \frac{1}{2}k_p(x_1 - x_d)^2$$

We measured the values of V immediately before and after the transition to evaluate whether energy was gained or lost during the jump. Figure 9 shows the energy profile at the jump points, while Figure 10 plots the change ΔV.

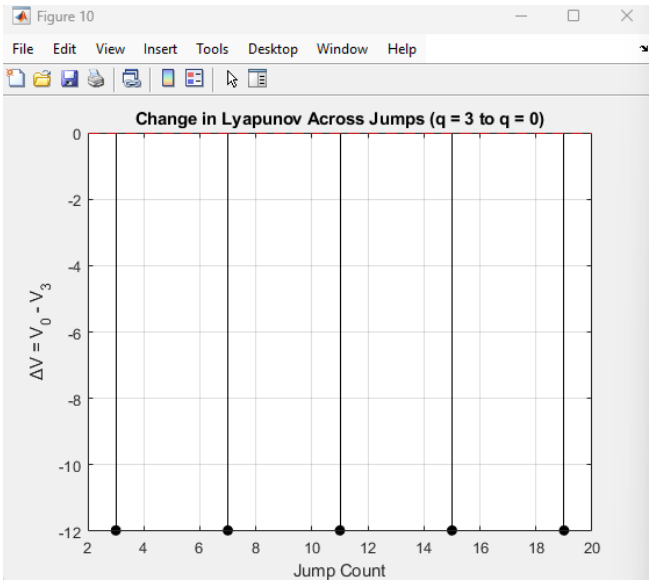

Fig. 10. Change ΔV across jumps $q = 3 \rightarrow q = 0$, showing mostly negative or near-zero values.

The data show that V typically decreases or remains approximately constant across these transitions. This behavior aligns with the physical interpretation of the system resetting its state after a ballistic return. While the decrease is not always strict, the absence of energy gain supports the practical repeatability and boundedness of hybrid trajectories.

G. Interpretation

The numerical results confirm that both Lyapunov functions and decrease during flows in their respective modes and across jump transitions. This hybrid Lyapunov structure supports the claim of practical stability and repeatable hybrid behavior in the control system.

In mode q = 3, although the Lyapunov function is not strictly decreasing, it reflects a consistent return toward the pre-contact configuration. Each cycle leads the system through energy injection (mode q=2) followed by passive return under gravity, where periodically rises and falls. This pattern supports the notion of convergence to a predictable reset state, altough not through conventional Lyapunov stability. The robot reliably returns to its initial condition, enabling repeatable task execution.

V. Simulation

To analyze the behavior of the proposed hybrid control scheme, we implemented the model in MATLAB using the HyEQ Toolbox [2]. The system was simulated over a hybrid time domain with a maximum of 25 flow seconds and 20 jumps. The initial condition was set to $x_1 = -1$, $x_2 = 0$, and $q = 0$, meaning the arm begins in free motion mode, far from the contact surface.

A. Mode Transitions and Force Logic

Transitions between the four discrete modes were defined based on contact force and velocity thresholds. The arm interacts with a compliant environment modeled via the Kelvin-Voigt [1] model. Force thresholds $\gamma = 3$ and $\delta = 0.5$ triggered the contact and release transitions, while the reset transition occurred once the position reached -1.

The jump map resets the timer and switches control modes accordingly:

- From position to force control when $f_c \geq \gamma$,
- From force control to throw when $f_c \in [f_d - \delta, f_d + \delta]$,
- From throw to reset when $x_2 \geq v_{\text{release}}$,
- From reset back to position control when $x_1 \leq -1$.

B. Simulation Results

Figure 11 shows the arm's position x_1 over hybrid time. We observe smooth convergence toward the contact region followed by a brief transition to force regulation and eventually a throwing motion. Figure 12 presents the velocity x_2, which clearly peaks during the throw execution phase.

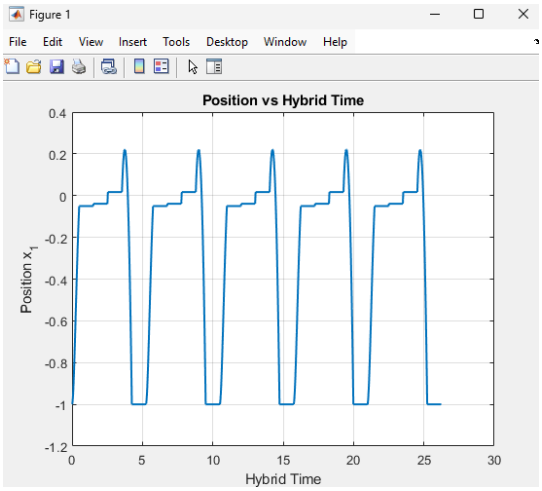

Fig. 11. Position x_1 vs. Hybrid Time

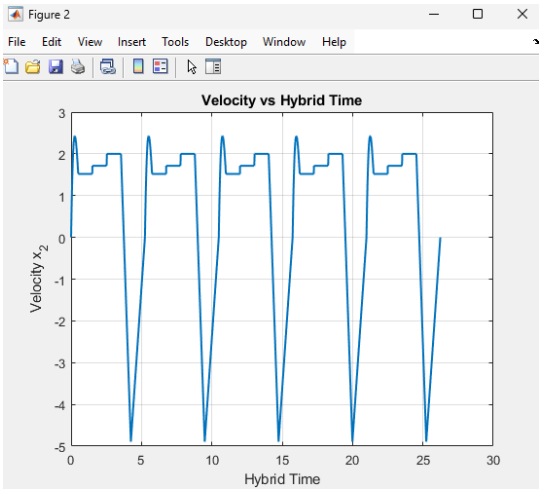

Fig. 12. Velocity x_2 vs. Hybrid Time

C. Phase Portrait and Mode Behavior

The phase portrait in Figure 13 shows the system trajectory in the (x_1, x_2) plane. The initial and final points are marked, and the trajectory curvature reflects the control mode transitions. A stair plot in Figure 14 illustrates the evolution of the discrete mode q, confirming that all four modes were reached during the simulation and the system correctly reset to begin a new cycle.

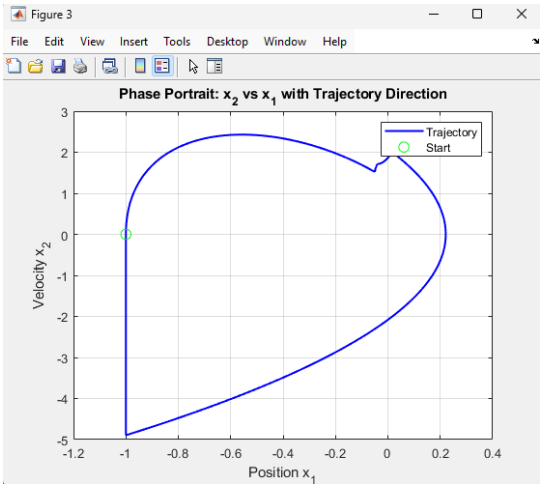

Fig. 13. Phase Portrait x_2 vs.x_1

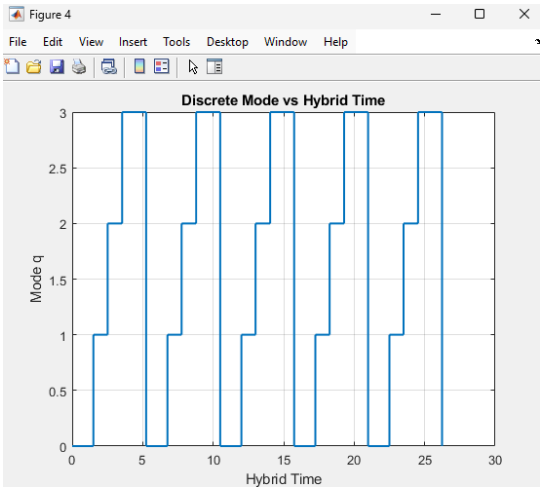

Fig. 14. Discrete Mode q vs. Hybrid Time

These results validate the hybrid control structure's ability to manage physical contact, force regulation, and dynamic transitions using hysteresis-based thresholds and jump conditions. The simulation also demonstrates that the full cycle, from approach to contact, throw, and reset is completed robustly and repeatably.

VI. Conclusion

This project presented a hybrid control framework for a robotic manipulator executing a pick-throw-reset cycle. By modeling the system as a hybrid dynamical system with four discrete modes, we successfully designed and analyzed mode-specific control laws using Lyapunov-based techniques.

For the position regulation and force control phases (modes $q = 0$, and $q = 1$), we proposed Lyapunov candidate functions and confirmed their decrease during flows via numerical simulations. We further verified that these functions decrease across discrete transitions, satisfying hybrid Lyapunov stability conditions. For mode $q = 2$, which injects energy for throwing, no Lyapunov function was proposed due to the intended destabilizing behavior. Mode $q = 3$, which models passive ballistic motion under gravity, was shown to exhibit convergence to the pre-contact configuration using a modified Lyapunov-like function, validating practical repeatability of the hybrid task cycle.

Our analysis confirms that the hybrid system satisfies the hybrid basic conditions, ensuring nominal well-posedness per Theorem 6.8 [3]. This guarantees robust solution behavior and consistent execution of hybrid trajectories.

Overall, the report demonstrates how hybrid systems theory enables formal verification of complex robotic behaviors involving both continuous dynamics and discrete mode transitions. This structure is essential for reliable task execution in systems involving impacts, resets, or contact regulation.

References

[1] R. Carloni, R. G. Sanfelice, A. R. Teel, and C. Melchiorri, "A hybrid control strategy for robust contact detection and force regulation," in *Proceedings of the American Control Conference (ACC)*, 2007, p. 1461–1466.

[2] R. G. Sanfelice, "Hybrid equations toolbox (hyeq toolbox) version 3.0," https://github.com/pnanez/HyEQ_Toolbox, 2022, mATLAB toolbox for simulating hybrid dynamical systems.

[3] R. Goebel, R. G. Sanfelice, and A. R. Teel, *Hybrid Dynamical Systems: Modeling, Stability, and Robustness*. Princeton, NJ: Princeton University Press, 2012.